JSAP1 and JLP are required for ARF6 localization to the midbody in cytokinesis

Baljinnyam Tuvshintugs[1,†], Tokiharu Sato[1,†], Radnaa Enkhtuya[1], Katsumi Yamashita[2], and Katsuji Yoshioka[1,*]

[1]*Division of Molecular Cell Signaling, Cancer Research Institute, Kanazawa University, Kanazawa 920-1192, Japan*
[2]*Division of Pharmaceutical Sciences, Institute of Medical, Pharmaceutical and Health Sciences, Kanazawa University, Kanazawa 920-1192, Japan*

Abstract.

The ADP-ribosylation factor 6 (ARF6) GTPase is important in cytokinesis, and localizes to the midbody. However, the mechanism and regulation of ARF6's recruitment to the midbody are largely unknown. Here, we investigated the functions of two binding partners of active ARF6, c-Jun NH_2-terminal kinase (JNK)/stress-activated protein kinase-associated protein 1 (JSAP1) and JNK-associated leucine zipper protein (JLP), by gene knockout and rescue experiments in mouse embryonic fibroblasts. Depleting both JSAP1 and JLP impaired ARF6's localization to the midbody and delayed cytokinesis. These defects were almost completely rescued by wild-type JSAP1 or JLP, but not by JSAP1 or JLP mutants that were unable to interact with active ARF6 or with the kinesin heavy chain (KHC) of kinesin-1. In transfected cells, a constitutively active form of ARF6 associated with KHC only when coexpressed with wild-type JSAP1 or JLP, and not with a JSAP1 or JLP mutant. These findings suggest that JSAP1 and JLP, which might be paralogous to each other, are critical and functionally redundant in cytokinesis, and control ARF6 localization to the midbody by forming a tripartite complex of JSAP1/JLP, active ARF6, and kinesin-1.

Keywords: ARF6, cytokinesis, kinesin, mouse embryonic fibroblast, small GTPase

Cytokinesis is the final stage of cell division, in which a single cell is physically separated into two daughter cells. The failure of cytokinesis can lead to aneuploidy, which is often associated with cancer. There is growing evidence that membrane trafficking plays an important role during cytokinesis in animal cells (Albertson *et al*. 2005; Montagnac *et al*. 2008). Although several small GTPases, including ADP-ribosylation factor 6 (ARF6), are known to regulate membrane trafficking during cytokinesis (D'Souza-Schorey & Chavrier 2006; Schweitzer *et al*. 2011; Schiel & Prekeris 2013), the mechanisms that control these GTPases spatiotemporally are not well understood. ARF6, like other small GTPases, cycles between an active GTP-bound and an inactive GDP-bound state. Recent studies have shown that ARF6 is crucial for proper cytokinesis, and that it localizes to the midbody, a narrow intercellular bridge connecting two daughter cells (Chesneau *et al*. 2012; Makyio *et al*. 2012).

C-Jun NH_2-terminal kinase (JNK)/stress-activated protein kinase-associated protein 1 (JSAP1, also known as JIP3 or Sunday Driver) was originally identified as a binding protein for JNK, and was suggested to function as a scaffold in mammalian JNK signaling pathways (Ito *et al*. 1999; Kelkar *et al*. 2000). Subsequent genetic studies supported JSAP1's role as a scaffold protein (Kelkar *et al*. 2003; Ha *et al*. 2005). In addition, recent studies have indicated that JSAP1 plays key roles in several neuronal processes, including axon elongation and branching (Suzuki *et al*. 2010; Bilimoria *et al*. 2010; Sun *et al*. 2013). The JNK-associated leucine zipper protein (JLP, also known as JIP4 or SPAG9) is closely related in structure to JSAP1, and can organize JNK and p38 mitogen-activated protein kinase signaling pathways (Lee *et al*. 2002; Kelkar *et al*. 2005). This scaffold protein is reported to be important in myoblast differentiation (Takaesu *et al*. 2006; Kang *et al*. 2008). *Jsap1* and *Jlp* might be paralogous to each other. To date, however, whether JSAP1 and JLP have overlapping functions remains largely unknown.

JSAP1 and JLP have also been identified as kinesin light chain (KLC)-binding proteins, and are thought to function as adaptor proteins that link cargos to kinesin-1 (Verhey *et al*. 2001; Nguyen *et al*. 2005), which is a heterotetramer of two kinesin heavy chains (KHC) and two KLC subunits. KHC includes a globular ATP-binding motor domain. Recently, JSAP1 and JLP were identified as binding partners for active ARF6 (Montagnac *et al*. 2009; Suzuki *et al*. 2010). Montagnac *et al*. reported that active ARF6 binds to JSAP1/JLP and negatively regulates the association of JSAP1/JLP with kinesin-1. In this study, we investigated the functions of JSAP1 and JLP by gene knockout (KO) and rescue experiments in mouse embryonic fibroblasts (MEFs). Our findings suggest that JSAP1 and JLP play critical, functionally redundant roles in cytokinesis by controlling ARF6's localization to the midbody as part of a tripartite complex of JSAP1/JLP, active ARF6, and kinesin-1.

Results

Phenotypic analysis of Jsap1 KO, Jlp KO, and Jsap1:Jlp double-KO (dKO) MEFs

To examine the roles of JSAP1 and JLP in proliferating cells, we used wild-type and mutant mouse MEFs carrying *loxP*-flanked (floxed) *Jsap1* and/or *Jlp* alleles, which allow a target gene to be disrupted by an adenovirus vector expressing Cre recombinase (AxCANCre). The disruption of *Jsap1* and *Jlp* by AxCANCre was confirmed by immunoblotting at 24 h post-infection (hpi). JSAP1 and JLP were not detected in AxCANCre-infected $Jsap1^{f/f}$ or $Jlp^{f/f}$ MEFs, respectively (Fig. 1A, lanes 2 and 3), and neither protein was detected in AxCANCre-infected $Jsap1^{f/f}$:$Jlp^{f/f}$ MEFs (lane 4).

We first investigated whether JSAP1 and/or JLP are required for MEF proliferation. Equal numbers of wild-type or each mutant MEF were plated at low density, and the number of adherent MEFs was measured by 4',6-diamidino-

†These authors contributed equally to the work.
*Correspondence: katsuji@staff.kanazawa-u.ac.jp

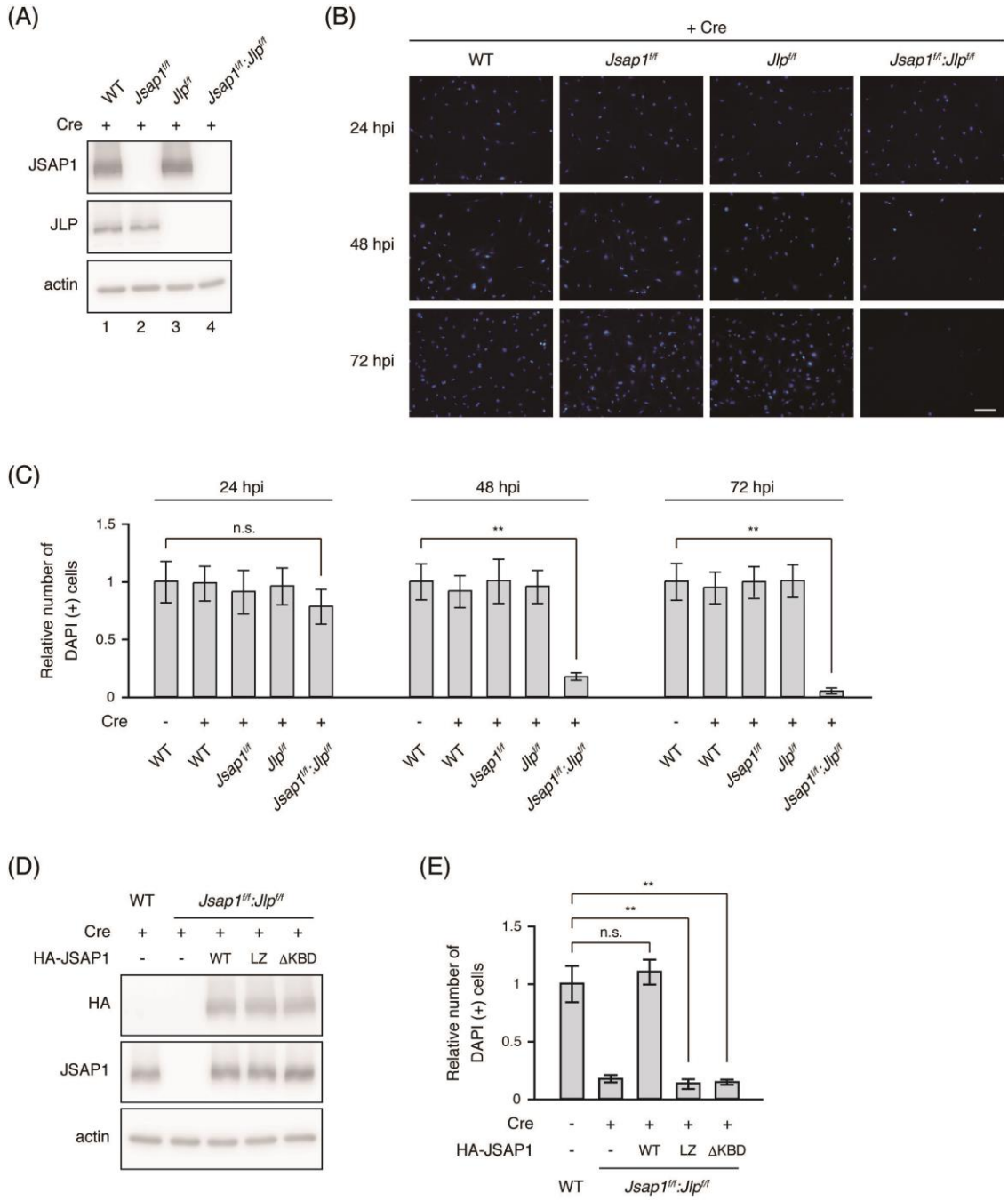

Figure 1. Phenotypic analysis of *Jsap1* KO, *Jlp* KO, and *Jsap1:Jlp* dKO MEFs. (A) Cre-induced deletion of *Jsap1* and *Jlp* in MEFs. Wild-type (WT), *Jsap1*$^{f/f}$, *Jlp*$^{f/f}$, and *Jsap1*$^{f/f}$*:Jlp*$^{f/f}$ MEFs infected with AxCANCre were analyzed at 24 hpi by immunoblotting with anti-JSAP1 and anti-JLP Abs. Actin was used as a loading control. (B) MEFs were infected with AxCANCre, and the number of DAPI-positive adherent MEFs was counted at the indicated times. (C) Quantification of the results in **B**. (D) *Jsap1*$^{f/f}$*:Jlp*$^{f/f}$ MEFs infected with lentiviruses expressing HA-JSAP1-WT, -LZ, or -ΔKBD were further infected with AxCANCre and were analyzed 24 h later by immunoblotting, as in **A**. WT MEFs were used as a control. (E) The number of DAPI-positive adherent MEFs expressing the indicated HA-JSAP1s was counted 48 h after infection with AxCANCre; results were quantified as in **C**. Values are the mean ± SEM from three independent experiments; n.s., not significant; $^{**}P < 0.01$; scale bar, 200 μm.

2-phenylindole (DAPI) staining at 24, 48, and 72 hpi (Fig. 1B and C). While Cre-induced *Jsap1* and *Jlp* single-KO MEFs grew normally and the number of adherent cells was similar to that in wild-type MEFs at each time point examined, the number of adherent *Jsap1:Jlp* dKO MEFs was markedly reduced at 48 and 72 hpi, but not at 24 hpi (Fig. 1B and C). We next conducted rescue experiments using wild-type and altered forms of JSAP1, including a deletion mutant lacking the KHC-binding domain (KBD) (Sun *et al*. 2011) and a mutant that could not interact with GTP-bound active ARF6 due to substitutions in the leucine zipper domain (Montagnac *et al*. 2009; Suzuki *et al*. 2010, see also Fig. 3 and Fig. S5 in Supporting Information). Lentiviral vectors were used to express these wild-type and mutant JSAP1 forms as hemagglutinin (HA)-tagged proteins (designated HA-JSAP1-WT, -LZ, and -ΔKBD) in the *Jsap1:Jlp* dKO MEFs. The lentiviral vector-mediated expression of the HA-JSAP1 proteins in dKO MEFs was comparable to that of endogenous

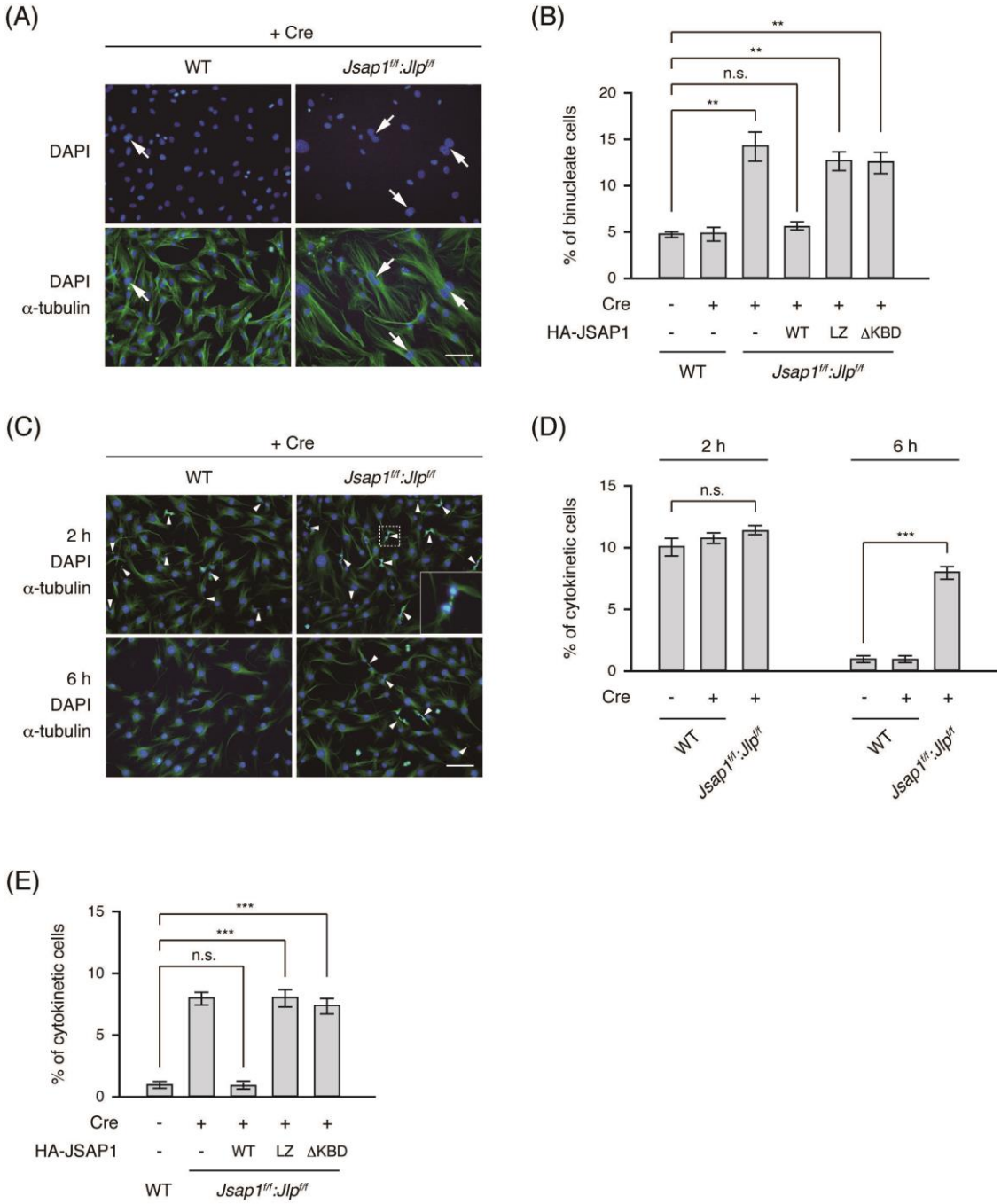

Figure 2. Delayed cytokinesis in *Jsap1:Jlp* dKO MEFs. (A,B) WT and *Jsap1*$^{f/f}$*:Jlp*$^{f/f}$ MEFs expressing the indicated HA-JSAP1s were infected with AxCANCre. At 36 hpi, the cells were stained with DAPI and α-tubulin, and the number of binucleate cells (arrows) in WT and dKO MEFs expressing the indicated HA-JSAP1s was counted. (C) Cytokinetic cells (arrowheads) in MEFs. WT and *Jsap1*$^{f/f}$*:Jlp*$^{f/f}$ MEFs infected with AxCANCre were treated with RO-3306. The MEFs were released from RO-3306 at 24 hpi and were stained with DAPI (blue) and anti-α-tubulin Ab (green) at the indicated time points after the release. Inset shows a magnified view of the dashed boxed area. (D) Quantification of the results in **C**. (E) Delayed cytokinesis in dKO MEFs was rescued by the expression of HA-JSAP1-WT, but not of HA-JSAP1-LZ or -ΔKBD. Cytokinetic cells in dKO MEFs expressing the indicated HA-JSAP1s were counted 6 h after the cells were released from RO-3306. For each experiment, 200-1000 cells and 200-400 cells were counted for the analysis of binucleate and cytokinetic cells, respectively. Values are the mean ± SEM from three independent experiments; n.s., not significant; $^{**}P < 0.01$; $^{***}P < 0.001$; scale bars, 100 μm.

JSAP1 in wild-type MEFs (Fig. 1D). Although HA-JSAP1-WT almost completely reversed the reduced numbers of dKO MEF cells, neither the HA-JSAP1-LZ nor the ΔKBD mutant was able to rescue the defect (Fig. 1E). Similar results were obtained with lentiviruses expressing HA-JLP-WT, -LZ, or -ΔKBD (Fig. S1 in Supporting Information). Taken together, these results suggest that JSAP1 and JLP are functionally redundant and play an important role in cell proliferation through interactions with kinesin-1 and ARF6.

Delayed cytokinesis in Jsap1:Jlp dKO MEFs

While analyzing the MEFs by DAPI staining, we noticed that the proportion of binucleate cells appeared to be higher in the *Jsap1:Jlp* dKO MEFs than in the wild-type

MEFs. We found that the frequency of binucleate cells at 36 hpi was 3 times higher in the dKO MEFs than in wild-type MEFs (Fig. 2A and B). This percentage of binucleate cells in the dKO MEFs may actually be underestimated, because many of the dKO MEFs had detached from the plates during culture, and the proportion of adherent dKO MEFs at 36 hpi was around 30% of that in wild-type MEFs (T. Sato and K. Yoshioka, unpublished data). We conducted rescue experiments with lentiviruses expressing HA-JSAP1-WT, -LZ, or -ΔKBD, and HA-JLP-WT, -LZ, or -ΔKBD. As shown in Fig. 2B (and Fig. S2 in Supporting Information), HA-JSAP1/JLP-WT, but not HA-JSAP1/JLP-LZ or -ΔKBD, reversed the increased frequency of binucleate cells. We next investigated whether ablating JSAP1 and JLP in MEFs would lead to defective cytokinesis. Uninfected wild-type MEFs and AxCANCre-infected wild-type and *Jsap1*$^{f/f}$*:Jlp*$^{f/f}$ MEFs were cultured in the presence of RO-3306, a selective cyclin-dependent kinase 1 (CDK1) inhibitor (Vassilev *et al*. 2006), to arrest the cell cycle at the G_2/M phase. The inhibitor was released at 24 hpi, and the arrested MEFs were allowed to enter mitosis with a large population of cells at the G_2/M phase (Fig. S3 in Supporting Information). Cells in cytokinesis were identified by the presence of the midbody (Fig. 2C). We found comparable proportions of dKO MEFs and AxCANCre-infected or -uninfected wild-type MEFs in cytokinesis 2 h after releasing the RO-3306 block (Fig. 2D, left). Six hours after release, the percentage of wild-type cells undergoing cytokinesis had severely decreased, whereas many dKO MEFs were still in cytokinesis (Fig. 2D, right). The lentivirus-mediated expression of HA-JSAP1/JLP-WT, but not of HA-JSAP1/JLP-LZ or -ΔKBD, reversed the increased proportion of cytokinetic cells in the dKO MEFs (Fig. 2E and Fig. S4 in Supporting Information). Collectively, these results suggest that JSAP1 and JLP regulate cytokinesis through their interactions with kinesin-1 and ARF6, and that the depletion of JSAP1 and JLP delays cytokinesis.

Tripartite complex formation of JSAP1/JLP, ARF6, and kinesin-1 KHC

JSAP1 and JLP are known to interact with active ARF6 and KHC. To determine whether JSAP1 forms a tripartite complex with ARF6 and kinesin-1 KHC, we transiently coexpressed HA-JSAP1 (WT, LZ, or ΔKBD) with a Flag-tagged, constitutively active ARF6 mutant (ARF6-Q67L-Flag) and Myc-tagged KHC (Myc-KHC) in human embryonic kidney (HEK) 293T cells. The cell lysates were then immunoprecipitated with an anti-HA antibody (Ab) and analyzed by immunoblotting with an anti-Flag or -Myc Ab (Fig. 3A). The results showed that HA-JSAP1-WT interacted with both ARF6-Q67L-Flag and Myc-KHC, HA-JSAP1-LZ interacted with Myc-KHC but not ARF6-Q67L-Flag, and HA-JSAP1-ΔKBD interacted with ARF6-Q67L-Flag but not Myc-KHC. Similar results were obtained with HA-JLP-WT, -LZ, and -ΔKBD (Fig. S5A in Supporting Information). We further assessed interactions between ARF6 and KHC in the presence or absence of JSAP1 by co-immunoprecipitation and immunoblotting assays in HEK 293T cells. Although ARF6-Q67L-Flag did not interact with Myc-KHC in the absence of HA-JSAP1-WT (Fig. 3B, lanes 3 and 7), ARF6-

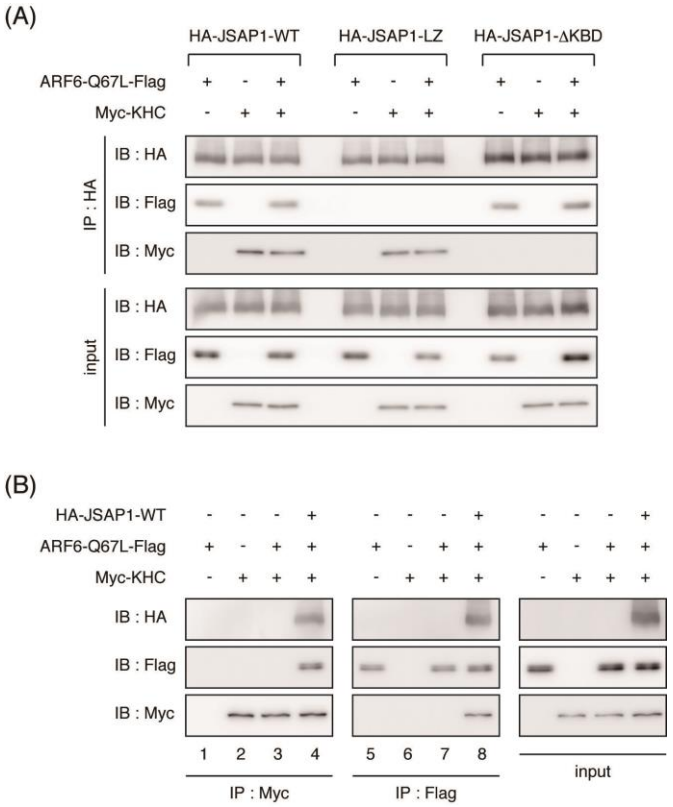

Figure 3. JSAP1 forms a tripartite complex with active ARF6 and KHC. HEK 293T cells were transiently transfected with various combinations of expression plasmids for HA-JSAP1-WT, (-LZ or -ΔKBD), ARF6-Q67L-Flag, and Myc-KHC as indicated. The cells were lysed, immunoprecipitated (IP) with anti-HA Ab (A), anti-Myc, or -Flag Ab (B), and analyzed by immunoblotting (IB) using anti-Flag, -Myc, or -HA Ab as indicated. The expression of HA-JSAP1s, ARF6-Q67L-Flag, or Myc-KHC in the total cell lysates is also shown (input).

Q67L-Flag and Myc-KHC were detected in precipitates with anti-Myc and -Flag Abs, respectively, in the presence of HA-JSAP1-WT (Fig. 3B, lanes 4 and 8). Similar results were obtained with HA-JLP-WT (Fig. S5B in Supporting Information). Taken together, these results indicate that JSAP1/JLP, ARF6, and KHC can form a tripartite complex.

Impaired localization of ARF6 to the midbody in Jsap1:Jlp dKO MEFs

ARF6 is known to localize to the midbody during cytokinesis. To test our hypothesis that JSAP1 and JLP are required for targeting ARF6 to the midbody, we compared the localization of endogenous ARF6 in wild-type and dKO MEFs. AxCANCre-infected wild-type and *Jsap1*$^{f/f}$*:Jlp*$^{f/f}$ MEFs were cultured in the presence of RO-3306. The MEFs were released from the RO-3306 block at 24 hpi, and were stained with an Ab against ARF6 2 h later (Fig. 4). A large proportion of the acetyl-α-tubulin-positive intercellular bridges in the wild-type MEFs were stained by the anti-ARF6 Ab. The percentage of intercellular bridges stained for ARF6 was sharply decreased in the dKO MEFs; this decrease was reversed WT, but not of HA-JSAP1/JLP-LZ or –ΔKBD (Fig. 4B and Fig. S6 in Supporting Information).

We next investigated whether ARF6's localization to the midbody is dependent on its interaction with JSAP1/JLP. ARF6-Q67L-Flag or a variant that could not interact specifically with JSAP1/JLP due to the additional point

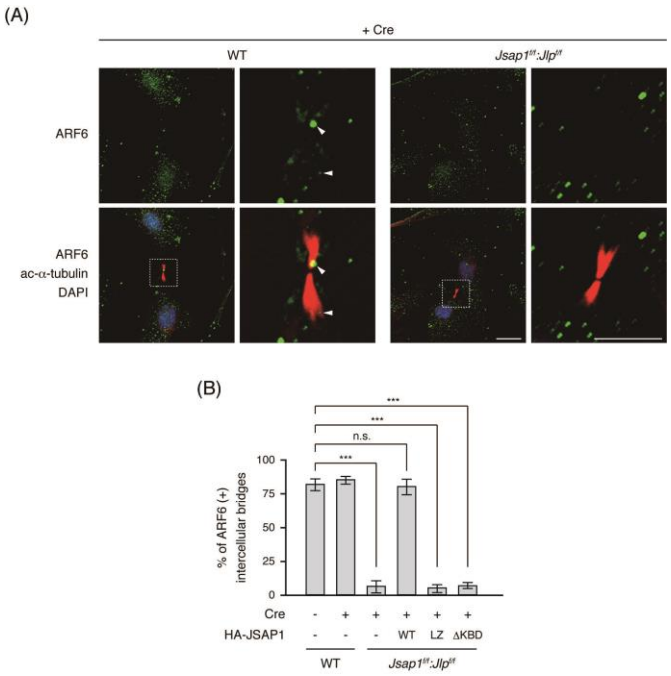

Figure 4. The localization of ARF6 to the midbody is impaired in *Jsap1:Jlp* dKO MEFs. (A) WT and *Jsap1*$^{f/f}$*:Jlp*$^{f/f}$ MEFs infected with AxCANCre were treated with RO-3306. The MEFs were released from RO-3306 at 24 hpi and immunostained with anti-ARF6 (green) and anti-acetyl (ac)-α-tubulin (red) Abs 2 h later. Nuclei were stained with DAPI (blue). Arrowheads indicate endogenous ARF6 localized to intercellular bridges. (B) The number of ARF6-positive intercellular bridges in the MEFs in **A** and in dKO MEFs lentivirally expressing the indicated HA-JSAP1s were counted as in **A**. Twenty intercellular bridges were analyzed per experiment. Values are the mean ± SEM from three independent experiments; n.s., not significant; ***P < 0.001; scale bars, 20 μm.

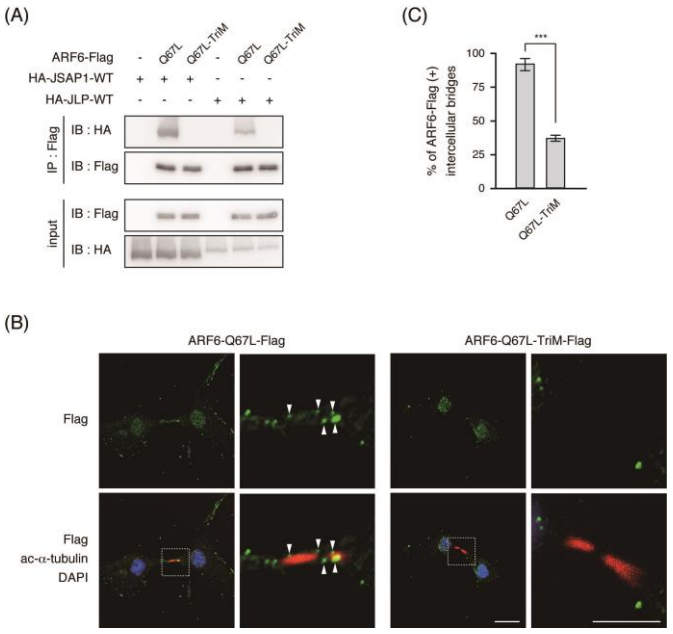

Figure 5. The localization of active ARF6 to the midbody requires its interaction with JSAP1/JLP. (A) Interaction of HA-JSAP1/JLP-WT with ARF6-Q67L-Flag or ARF6-Q67L-TriM-Flag. HEK 293T cells were transiently transfected with various combinations of expression plasmids, as indicated. The cells were lysed, immunoprecipitated (IP) with anti-Flag Ab, and analyzed by immunoblotting (IB) using anti-Flag or anti-HA Abs as indicated. The HA-JSAP1/JLP-WT, ARF6-Q67L-Flag, or ARF6-Q67L-TriM-Flag expressed in the total cell lysates is also shown (input). (B) Localization of ARF6-Q67L-Flag and ARF6-Q67L-TriM-Flag in MEFs. AxCANCre-infected WT MEFs expressing ARF6-Q67L-Flag or ARF6-Q67L-TriM-Flag were treated with RO-3306, were released from RO-3306 at 24 hpi, and were immunostained with anti-Flag (green) and anti-ac-α-tubulin (red) Abs 2 h later. Nuclei were stained with DAPI (blue). The right-hand panels in "ARF6-Q67L-Flag" and "ARF6-Q67L-TriM-Flag" show magnified views of the boxed region indicated in the left panels. Arrowheads indicate ARF6-Q67L-Flag that is localized to the intercellular bridge. (C) Quantification of the results in **B**. Twenty intercellular bridges were analyzed per experiment. Values are the mean ± SEM from three independent experiments; ***P < 0.001; scale bars, 20 μm.

mutations T53E, K58C, and N60T (Suzuki *et al.* 2010), designated ARF6-Q67L-TriM-Flag, was coexpressed with either HA-JSAP1-WT or HA-JLP-WT in HEK 293T cells. We confirmed that HA-JSAP1/JLP-WT interacted with ARF6-Q67L-Flag, but not with ARF6-Q67L-TriM-Flag (Fig. 5A). We next used lentiviruses to express ARF6-Q67L-Flag and ARF6-Q67L-TriM-Flag in wild-type MEFs, and analyzed the localization of these proteins by immunofluorescence. The vast majority of acetyl-α-tubulin-positive intercellular bridges in the cells expressing ARF6-Q67L-Flag were Flag-positive, but the frequency of ARF6 localization to the intercellular bridges was severely decreased in cells expressing ARF6-Q67L-TriM-Flag (Fig. 5B and C).

Collectively, these results suggest that active ARF6 localizes to the midbody through kinesin-1-dependent interactions with JSAP1/JLP.

Discussion

In the present study, we explored the roles of JSAP1 and JLP in dividing cells. We found that JSAP1 and JLP are functionally redundant, and that the depletion of both proteins causes cytokinesis to fail. We propose that JSAP1 and JLP regulate ARF6's localization to the midbody by forming a tripartite complex of JSAP1/JLP, active ARF6, and kinesin-1 KHC. This proposal is supported by the following lines of evidence: The *Jsap1:Jlp* dKO MEFs exhibited an increased percentage of binucleate cells and delayed cytokinesis, which were both almost completely rescued by the expression of wild-type JSAP1 or JLP (JSAP1/JLP-WT), whereas JSAP1 or JLP mutants that could not interact with active ARF6 (JSAP1/JLP-LZ) or KHC (JSAP1/JLP-ΔKBD) failed to reverse the defects (Fig. 2 and Figs. S2 and S4 in Supporting Information). In transfected cells, the association of a constitutively active ARF6 mutant (ARF6-Q67L) and KHC was observed only with the co-expression of JSAP1/JLP-WT, but not JSAP1/JLP-LZ or JSAP1/JLP-ΔKBD (Fig. 3 and Fig. S5 in Supporting Information). In addition, the localization of endogenous ARF6 to the midbody was impaired in *Jsap1:Jlp* dKO MEFs, and this impairment was reversed by the expression of JSAP1/JLP-WT, but not of JSAP1/JLP-LZ or JSAP1/JLP-ΔKBD (Fig. 4 and Fig. S6 in Supporting Information). Finally, in wild-type MEFs, ARF6-Q67L localized to the midbody with high frequency, consistent with previous reports (Schweitzer & D'Souza-Schorey 2002; Makyio *et al.* 2012), but this midbody localization was severely impaired by introducing three additional point mutations that prevented ARF6-Q67L's interaction with JSAP1/JLP (Fig. 5). These data collectively suggest that JSAP1 and JLP function as adaptors that link

active ARF6 and kinesin-1.

Our findings are inconsistent with a previous study by Montagnac *et al*. (2009), which reported that ARF6-Q67L's binding to JSAP1/JLP interferes with the association of JSAP1/JLP and kinesin-1 KHC. This apparent discrepancy may be explained by the different experimental systems used, and by differences in interpretation of the results. We used a co-immunoprecipitation system in which ARF6-Q67L and KHC were transiently coexpressed with JSAP1/JLP-WT, -LZ, or -ΔKBD in mammalian cells, and then ARF6-Q67L, KHC, and JSAP1/JLP were precipitated and their interactions evaluated by immunoblotting (Fig. 3 and Fig. S5 in Supporting Information). Montagnac *et al*. used a glutathione S-transferase (GST) pull-down system, in which KHC was pulled down from mammalian cells with a GST fusion protein containing the JLP leucine zipper domain, which is responsible for interactions with KLC and active ARF6, in the presence of ARF6-Q67L. This system pulls KHC down through its interaction with KLC. Montagnac *et al*. reported that ARF6-Q67L and KLC bind competitively to JSAP1/JLP; they showed that the amount of KHC pulled down decreased as the ARF6-Q67L concentration increased. These results, however, do not necessarily support the proposal that ARF6-Q67L binding to JSAP1/JLP negatively controls the association of JSAP1/JLP with kinesin-1 KHC.

To date, no interaction has been shown between JSAP1/JLP and guanine nucleotide exchange factors (GEFs) for ARF6, which catalyze the transition from the inactive, GDP-bound ARF6 to an active, GTP-bound ARF6. Thus, ARF6 is probably activated independently from JSAP1/JLP, and later forms part of the tripartite complex. It was recently reported that ARF6 is transiently associated with the ingressing cleavage furrow when activated by its GEF EFA6, and is subsequently targeted to the Flemming body, the central region of the midbody, during late cytokinesis (Makyio *et al*. 2012; Ueda *et al*. 2013). JSAP1/JLP might load activated ARF6 at the cleavage furrow and transport it to the midbody in collaboration with kinesin-1. Further study is needed to investigate the spatiotemporal changes of JSAP1 and JLP during cytokinesis.

Materials and Methods

Mice. All experimental procedures involving mice were approved by the Institutional Animal Care and Use Committee of Kanazawa University. *Jsap1*$^{f/f}$ mice were generated previously (Iwanaga *et al*. 2007). The generation of mice carrying floxed alleles of *Jlp* will be described elsewhere in detail. Briefly, two *lox*P sites were inserted into the intronic regions flanking exon 5 of the *Jlp* gene. Heterozygous mice (*Jlp*$^{f/+}$) were crossed with *Jsap1*$^{f/+}$ mice to generate *Jsap1*$^{f/+}$:*Jlp*$^{f/+}$ mice. These mutant mice were backcrossed to C57BL/6 for more than ten generations, and the resulting mice were used in this study. C57BL/6 mice were obtained from Japan SLC (Hamamatsu, Japan).

Cell cultures. MEFs were prepared from 14.5-day-old embryos from wild-type C57BL/6, *Jsap1*$^{f/f}$, *Jlp*$^{f/f}$, and *Jsap1*$^{f/f}$:*Jlp*$^{f/f}$ mice. After removing the heads and internal organs, the embryos were minced, trypsinized, and re-suspended in Dulbecco's modified Eagle's medium (Sigma-Aldrich, St. Louis, MO, USA) containing 10% fetal bovine serum. MEFs were used until passage 5. HEK 293T cells were cultured as described previously (Bayarsaikhan *et al*. 2007). In some experiments, RO-3306 (10 μM, Santa Cruz Biotechnology, Santa Cruz, CA, USA) was dissolved in dimethyl sulfoxide (DMSO) and added to the culture medium (see figure legends).

Plasmids. The mammalian expression plasmid pCL20c-CMV-HA-JSAP1-WT was described previously (Sato *et al*. 2008). The coding sequence for full-length JSAP1 with four leucine-to-alanine substitutions (at residues 431, 438, 445, and 452), a deletion mutant of JSAP1 KBD (residues 51-81), full-length mouse JLP (Iwanaga *et al*. 2008), full-length JLP with four leucine-to-alanine substitutions (at residues 406, 413, 420, and 427), or a deletion mutant of JLP KBD (residues 45-75), was inserted into pCL20c-CMV-HA to generate pCL20c-CMV-HA-JSAP1-LZ, -JSAP1-ΔKBD, -JLP-WT, -JLP-LZ, and -JLP-ΔKBD, respectively. To generate pCL20c-ARF6-Q67L-Flag and -ARF6-Q67L-TriM-Flag, we subcloned the coding regions of full-length mouse ARF6 (NM_007481) with either one substitution (Q67L) or four substitutions (T53E, K58C, N60T, and Q67L) and a Flag tag sequence at the 3' end into pCL20c-CMV. These coding sequences were also inserted into pcDNA3 (Life Technologies, Carlsbad, CA, USA) to generate the expression plasmids pcDNA3-ARF6-Q67L-Flag and -ARF6-Q67L-TriM-Flag. The coding region for full-length mouse KHC (NM_008449) with a Myc tag sequence at the 5' end was inserted into pcDNA3. The resultant plasmid was designated pcDNA3-Myc-KHC. Substitutions and deletions in cDNAs were introduced by overlapping polymerase chain reaction (PCR), as described previously (Ito *et al*. 1999). All PCR products were verified by sequencing.

Viral infection and DAPI-staining analysis. To generate *Jsap1* KO, *Jlp* KO, or *Jsap1:Jlp* dKO MEFs, the corresponding MEFs were infected with AxCANCre (a gift from I. Saito). For DAPI staining, MEFs were plated in 12-well plates at 5 x 10^3 cells per well and were infected with AxCANCre. The medium containing the virus was removed at 2.5 hpi, and the MEFs were washed twice with fresh medium and then cultured in fresh medium. At 24, 48, and 72 hpi, the MEFs were washed once with phosphate-buffered saline, fixed with 4% paraformaldehyde, and stained with DAPI (Sigma-Aldrich). DAPI-positive cells in five randomly chosen fields (1.4 mm^2 per field) were counted for each experiment. Images were captured with a fluorescence microscope (Olympus IX71, Olympus, Tokyo, Japan). The pCL20c series of lentiviral vectors was produced as described previously (Sato *et al*. 2008). MEFs were infected with the lentiviruses at least three days before AxCANCre infection, and were used for rescue experiments.

Flow cytometry. MEFs were plated in 9-cm dishes at 1 x 10^5 cells per dish, and were cultured in the presence of either DMSO (vehicle) or RO-3306. MEFs were harvested after 22 h, and were fixed with 70% ethanol, treated with RNase A (Sigma-Aldrich), stained with propidium iodide (Sigma-Aldrich), and analyzed by a flow cytometer (FACSCanto II, BD Biosciences, San Jose, CA, USA).

Transfection, immunoprecipitation and immunoblotting. HEK 293T cells were plated in 35-mm dishes at 2 x 10^5 cells per dish, and were co-transfected with expression plasmids using polyethylenimine, essentially as described previously (Tanahashi *et al*. 2010). Twenty-four hours after transfection, the cells were lysed in lysis buffer (25 mM Tris-HCl pH 7.5, 1 mM EDTA, 5 mM $MgCl_2$, 10 mM KCl, and 1% TritonX-100) containing Protease Inhibitor Cocktail (Sigma-Aldrich), and were analyzed by immunoblotting as described previously (Sato *et al*. 2004) using the following Abs: rabbit polyclonal anti-JSAP1 (0.33 μg/ml; Miura *et al*. 2006), rabbit polyclonal anti-JLP (2 μg/ml; Iwanaga *et al*. 2008), rat polyclonal anti-HA (1:5000; Roche, Basel, Switzerland), mouse monoclonal horseradish peroxidase (HRP)-conjugated anti-Flag M2 (1:1000; Sigma-Aldrich), mouse monoclonal anti-Myc (1:3000; Cell Signaling Technology, Beverly, MA, USA), and rabbit polyclonal anti-actin (1:1000; Sigma-Aldrich). The following secondary HRP-conjugated IgG Abs were used: sheep anti-mouse and donkey anti-rabbit (1:5000, both from GE Healthcare, Buckinghamshire, UK),

and goat anti-rat (1:5000, Santa Cruz Biotechnology). Protein bands were visualized using the Immobilon Western Chemiluminescence system (Millipore, Bedford, MA, USA). To analyze protein-protein interactions, cell lysates (prepared as described above) were immunoprecipitated with rat polyclonal anti-HA (1:500; Roche), mouse monoclonal anti-Flag M2 (1:1000; Sigma-Aldrich), or mouse monoclonal anti-Myc (1:1000; Cell Signaling Technology) Abs bound to protein G-Sepharose (GE Healthcare) beads, and were analyzed by immunoblotting.

Immunocytochemistry. For immunocytochemical analysis, MEFs were plated onto glass cover slips (Thermo Fisher Scientific, Waltham, MA, USA) in 12-well plates at 5 x 10^3 cells per well. The MEFs were left uninfected or were infected with AxCANCre and/or lentiviruses, as indicated in the figures. To quantify binucleate cells, MEFs were fixed at 36 h after infection with AxCANCre. To analyze the number of cytokinetic cells, MEFs were treated with the CDK1 inhibitor RO-3306, were released from the inhibitor, and were fixed at the time points indicated in the figure legends. The fixed MEFs were stained with DAPI and mouse monoclonal anti-α-tubulin Ab (1:2000; Sigma-Aldrich). To analyze ARF6's localization during cytokinesis, MEFs were cultured in the presence of RO-3306, fixed 2 h after the RO-3306 blockade was released, and immunostained with rabbit monoclonal anti-acetyl-α-tubulin (1:1500; Cell Signaling) and either mouse monoclonal anti-ARF6 (1:100; Santa Cruz Biotechnology) or mouse monoclonal anti-Flag M2 (1:2000; Sigma-Aldrich) Abs. The secondary Abs used were goat Alexa fluor 488-conjugated anti-mouse IgG and goat Alexa fluor 568-conjugated anti-rabbit IgG Abs (both diluted 1:1000; Life Technologies). Immunocytochemistry was performed by standard protocols as described previously (Sato *et al*. 2011). Images were captured with a confocal laser scanning microscope (LSM510; Zeiss, Oberkochem, Germany).

Statistical analysis. Significance was determined using a two-tailed unpaired Student's *t*-test. $P < 0.05$ was considered to be statistically significant.

Acknowledgements

We are grateful to I. Saito (University of Tokyo) for providing the AxCANCre. This work was supported in part by Grants-in-Aid from the Ministry of Education, Culture, Sports, Science and Technology of Japan.

References

Albertson, R., Riggs, B. & Sullivan, W. (2005) Membrane traffic: a driving force in cytokinesis. *Trends Cell Biol*. **15**, 92-101.

Bayarsaikhan, M., Takino, T., Gantulga, D., Sato, H., Ito, T. & Yoshioka, K. (2007) Regulation of N-cadherin-based cell-cell interaction by JSAP1 scaffold in PC12h cells. *Biochem. Biophys. Res. Commun*. **353**, 357-362.

Bilimoria, P.M., de la Torre-Ubieta, L., Ikeuchi, Y., Becker, E.B., Reiner, O. & Bonni, A. (2010) A JIP3-regulated GSK3β/DCX signaling pathway restricts axon branching. *J. Neurosci*. **30**, 16766-16776.

Chesneau, L., Dambournet, D., Machicoane, M., Kouranti, I., Fukuda, M., Goud, B. & Echard, A. (2012) An ARF6/Rab35 GTPase cascade for endocytic recycling and successful cytokinesis. *Curr. Biol*. **22**, 147-153.

D'Souza-Schorey, C. & Chavrier, P. (2006) ARF proteins: roles in membrane traffic and beyond. *Nat. Rev. Mol. Cell Biol*. **7**, 347-358.

Ha, H.Y., Cho, I.H., Lee, K.W., Lee, K.W., Song, J.Y., Kim, K.S., Yu, Y.M., Lee, J.K., Song, J.S., Yang, S.D., Shin, H.S. & Han, P.L. (2005) The axon guidance defect of the telencephalic commissures of the JSAP1-deficient brain was partially rescued by the transgenic expression of JIP1. *Dev. Biol.* **277**, 184-199

Ito, M., Yoshioka, K., Akechi, M., Yamashita, S., Takamatsu, N., Sugiyama, K., Hibi, M., Nakabeppu, Y., Shiba, T. & Yamamoto, K.I. (1999) JSAP1, a novel Jun N-terminal protein kinase (JNK) that functions as scaffold factor in the JNK signaling pathway. *Mol. Cell. Biol.* **19**, 7539-7548.

Iwanaga, A., Sato, T., Sugihara, K., Hirao, A., Takakura, N., Okamoto, H., Asano, M. & Yoshioka, K. (2007) Neural-specific ablation of the scaffold protein JSAP1 in mice causes neonatal death. *Neurosci. Lett.* **429**, 43-48.

Iwanaga, A., Wang, G., Gantulga, D., Sato, T., Baljinnyam, T., Shimizu, K., Takumi, K., Hayashi, M., Akashi, T., Fuse, H., Sugihara, K., Asano, M. & Yoshioka, K. (2008) Ablation of the scaffold protein JLP causes reduced fertility in male mice. *Transgenic Res.* **17**, 1045-1058.

Kang, J.S., Bae, G.U., Yi, M.J., Yang, Y.J., Oh, J.E., Takaesu, G., Zhou, Y.T., Low, B.C. & Krauss, R.S. (2008) A Cdo-Bnip-2-Cdc42 signaling pathway regulates p38alpha/beta MAPK activity and myogenic differentiation. *J. Cell Biol.* **182**, 497-507.

Kelkar, N., Gupta, S., Dickens, M. & Davis, R.J. (2000) Interaction of a mitogen-activated protein kinase signaling module with the neuronal protein JIP3. *Mol. Cell. Biol.* **20**, 1030-1043.

Kelkar, N., Delmotte, M.H., Weston, C.R., Barrett, T., Sheppard, B.J., Flavell, R.A. & Davis, R.J. (2003) Morphogenesis of the telencephalic commissure requires scaffold protein JNK-interacting protein 3 (JIP3). *Proc. Natl. Acad. Sci. USA* **100**, 9843-9848.

Kelkar, N., Standen, C.L. & Davis, R.J. (2005) Role of the JIP4 scaffold protein in the regulation of mitogen-activated protein kinase signaling pathways. *Mol. Cell. Biol.* **25**, 2733-2743.

Lee, C.M., Onésime, D., Reddy, C.D., Dhanasekaran, N. & Reddy, E.P. (2002) JLP: A scaffolding protein that tethers JNK/p38MAPK signaling modules and transcription factors. *Proc. Natl. Acad. Sci. USA* **99**, 14189-14194.

Makyio, H., Ohgi, M., Takei, T. *et al*. (2012) Structural basis for Arf6-MKLP1 complex formation on the Flemming body responsible for cytokinesis. *EMBO J.* **31**, 2590-2603.

Miura, E., Fukaya, M., Sato, T., Sugihara, K., Asano, M., Yoshioka, K. & Watanabe, M. (2006) Expression and distribution of JNK/SAPK-associated scaffold protein JSAP1 in developing and adult mouse brain. *J. Neurochem*. **97**, 1431-1446.

Montagnac, G., Echard, A. & Chavrier, P. (2008) Endocytic traffic in animal cell cytokinesis. *Curr. Opin. Cell Biol*. **20**, 454-461.

Montagnac, G., Sibarita, J.B., Loubéry, S., Daviet, L., Romao, M., Raposo, G. & Chavrier, P. (2009) ARF6 Interacts with JIP4 to control a motor switch mechanism regulating endosome traffic in cytokinesis. *Curr. Biol*. **19**, 184-195.

Nguyen, Q., Lee, C.M., Le, A. & Reddy, E.P. (2005) JLP associates with kinesin light chain 1 through a novel leucine zipper-like domain. *J. Biol. Chem.* **280**, 30185-30191.

Sato, S., Ito, M., Ito, T. & Yoshioka, K. (2004) Scaffold protein JSAP1 is transported to growth cones of neurites independent of JNK signaling pathways in PC12h cells. *Gene* **329**, 51-60.

Sato, T., Torashima, T., Sugihara, K., Hirai, H., Asano, M. & Yoshioka, K. (2008) The scaffold protein JSAP1 regulates proliferation and differentiation of cerebellar granule cell precursors by modulating JNK signaling. *Mol. Cell. Neurosci.* **39**, 569-578.

Sato, T., Enkhbat, A. & Yoshioka, K. (2011) Role of plasma membrane localization of the scaffold protein JSAP1 during differentiation of cerebellar granule cell precursors. *Genes Cells* **16**, 58-68.

Schiel, J.A. & Prekeris, R. (2013) Membrane dynamics during cytokinesis. *Curr. Opin. Cell Biol*. **25**, 92-98.

Schweitzer, J.K. & D'Souza-Schorey, C. (2002) Localization and activation of the ARF6 GTPase during cleavage furrow ingression and cytokinesis. *J. Biol. Chem*. **277**, 27210-27216.

Schweitzer, J.K., Sedgwick, A.E. & D'Souza-Schorey, C. (2011) ARF6-mediated endocytic recycling impacts cell movement, cell division and lipid homeostasis. *Semin. Cell Dev. Biol*. **22**, 39-47.

Sun, F., Zhu, C., Dixit, R. & Cavalli, V. (2011) Sunday Driver/JIP3 binds kinesin heavy chain directly and enhances its motility. *EMBO J.* **30**, 3416-3429.

Sun, T., Yu, N., Zhai, L.K., Li, N., Zhang, C., Zhou, L., Huang, Z., Jiang, X.Y., Shen, Y. & Chen, Z.Y. (2013) c-Jun NH2-terminal kinase (JNK)-interacting protein-3 (JIP3) regulates neuronal axon elongation in a kinesin- and JNK-dependent manner. *J. Biol. Chem.* **288**, 14531-14543.

Suzuki, A., Arikawa, C., Kuwahara, Y., Itoh, K., Watanabe, M., Watanabe, H., Suzuki, T., Funakoshi, Y., Hasegawa, H. & Kanaho, Y. (2010) The scaffold protein JIP3 functions as a downstream effector of the small GTPase ARF6 to regulate neurite morphogenesis of cortical neurons. *FEBS Lett*. **584**, 2801-2806.

Takaesu, G., Kang, J.S., Bae, G.U., Yi, M.J., Lee, C.M., Reddy, E.P. & Krauss, R.S. (2006) Activation of p38alpha/beta MAPK in myogenesis via binding of the scaffold protein JLP to the cell surface protein Cdo. *J. Cell Biol.* **175**, 383-388.

Tanahashi, H., Kito, K., Ito, T. & Yoshioka, K. (2010) MafB protein stability is regulated by the JNK and ubiquitin-proteasome pathways. *Arch. Biochem. Biophys*. **494**, 94-100.

Ueda, T., Hanai, A., Takei, T., Kubo, K., Ohgi, M., Sakagami, H., Takahashi, S., Shin, H.-W. & Nakayama, K. (2013) EFA6 activates Arf6 and participates in its targeting to the Flemming body during cytokinesis. *FEBS Lett.* **587**, 1617-1623.

Vassilev, L.T., Tovar, C., Chen, S., Knezevic, D., Zhao, X., Sun, H., Heimbrook, D.C. & Chen, L. (2006) Selective small-molecule inhibitor reveals critical mitotic functions of human CDK1. *Proc. Natl. Acad. Sci. USA* **103**, 10660-10665.

Verhey, K.J., Meyer, D., Deehan, R., Blenis, J., Schnapp, B.J., Rapoport, T.A. & Margolis, B. (2001) Cargo of kinesin identified as JIP scaffolding proteins and associated signaling molecules. *J. Cell Biol.* 152, 959-970.

Supporting Information

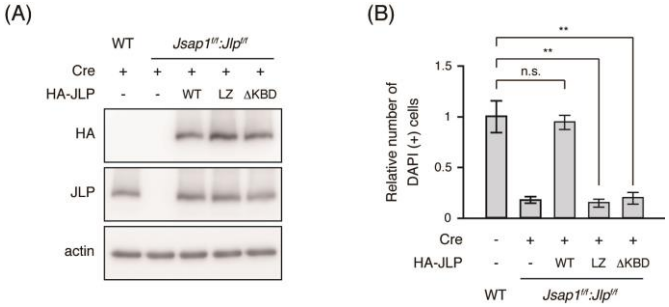

Figure S1. The decreased number of adherent *Jsap1:Jlp* dKO MEFs was rescued by JLP-WT, but not by JLP-LZ or JLP-ΔKBD. (A) Lentiviral-mediated expression of HA-JLP-WT, -LZ, and -ΔKBD. *Jsap1*$^{f/f}$*:Jlp*$^{f/f}$ MEFs infected with lentiviruses expressing the indicated HA-JLPs were further infected with AxCANCre, and were analyzed by immunoblotting at 24 hpi (see Fig. 1A). WT MEFs were used as a control. (B) Quantification of DAPI-positive MEFs expressing various HA-JLPs. DAPI-positive adherent MEFs expressing the indicated HA-JLPs were counted 48 h after infection with AxCANCre, and the results were quantified as in Fig. 1E. Values are the mean ± SEM from three independent experiments; n.s., not significant; ***P* < 0.01.

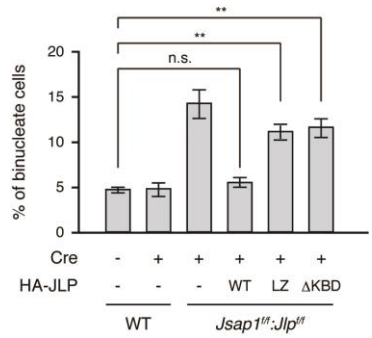

Figure S2. The increased proportion of binucleate cells in *Jsap1:Jlp* dKO MEFs was rescued by JLP-WT, but not by JLP-LZ or JLP-ΔKBD. *Jsap1*$^{f/f}$*:Jlp*$^{f/f}$ MEFs infected with lentiviruses expressing the indicated HA-JLPs were further infected with AxCANCre, were stained with DAPI and anti-α-tubulin Ab at 36 hpi, and the number of binucleate cells was counted for each type of MEF and quantified as in Fig. 2B. In each experiment, 200-1000 cells were counted. Values are the mean ± SEM from three independent experiments; n.s., not significant; ***P* < 0.01.

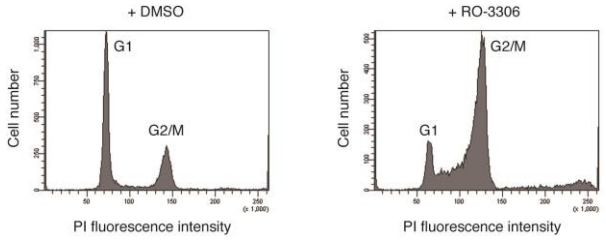

Figure S3. The cell cycle profile of MEFs treated with RO-3306. WT MEFs were cultured in the presence of either DMSO or RO-3306 and were analyzed by flow cytometry.

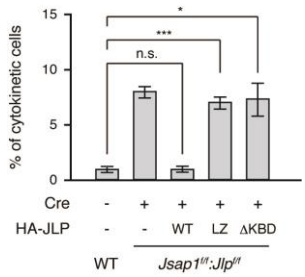

Figure S4. Delayed cytokinesis in *Jsap1:Jlp* dKO MEFs was rescued by JLP-WT, but not by JLP-LZ or JLP-ΔKBD. *Jsap1*$^{f/f}$*:Jlp*$^{f/f}$ MEFs infected with lentiviruses expressing the indicated HA-JLPs were further infected with AxCANCre, and were cultured in the presence of RO-3306. Cytokinetic cells were counted 6 h after the MEFs were released from RO-3306, and were quantified as in Fig. 2D. In each experiment, 200-400 cells were counted. Values are the mean ± SEM from three independent experiments; n.s., not significant; **P* < 0.05; ****P* < 0.001.

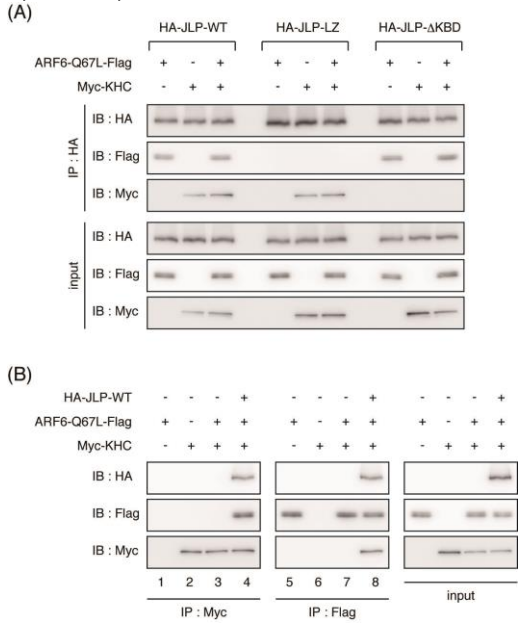

Figure S5. JLP forms a tripartite complex with active ARF6 and KHC. HEK 293T cells were transiently transfected with various combinations of expression plasmids for HA-JLP-WT, (-LZ or -ΔKBD), ARF6-Q67L-Flag, and Myc-KHC as indicated. The cells were lysed, were immunoprecipitated (IP) with anti-HA, (A) anti-Myc, or anti-Flag Ab (B), and were analyzed by immunoblotting (IB) using anti-Flag, -Myc, or -HA Ab as indicated. The expression of HA-JLPs, ARF6-Q67L-Flag, or Myc-KHC in total cell lysates is shown (input).

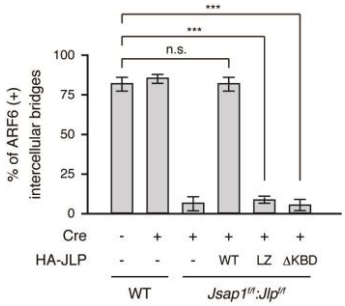

Figure S6. The impaired localization of ARF6 to the midbody in *Jsap1:Jlp* dKO MEFs was rescued by JLP-WT, but not by JLP-LZ or JLP-ΔKBD. *Jsap1*$^{f/f}$*:Jlp*$^{f/f}$ MEFs infected with lentiviruses expressing the indicated HA-JLPs were further infected with AxCANCre, cultured in the presence of RO-3306, and immunostained with anti-ARF6 and anti-acetyl-α-tubulin Abs 2 h after the release of RO-33. ARF6-positive intercellular bridges in the dKO MEFs were counted and quantified as in Fig. 4B. Twenty intercellular bridges were analyzed per experiment. Values are the mean ± SEM from three independent experiments; n.s., not significant; ****P* < 0.001.